Quasistatic X-Ray Speckle Metrology of Microscopic Magnetic Return-Point Memory

Michael S. Pierce,[1] Rob G. Moore,[1] Larry B. Sorensen,[1] Stephen D. Kevan,[2] Olav Hellwig,[3] Eric E. Fullerton,[3] and Jeffrey B. Kortright[4]

[1]*Department of Physics, University of Washington, Seattle, Washington 98195*
[2]*Department of Physics, University of Oregon, Eugene, Oregon 97403*
[3]*Hitachi Global Storage Technologies, San Jose, California 95120*
[4]*Lawrence Berkeley National Laboratory, Berkeley, California 94720*

(Received 11 July 2002; published 30 April 2003)

We have used coherent, resonant, x-ray magnetic speckle patterns to measure the statistical evolution of the microscopic magnetic domains in perpendicular magnetic films as a function of the applied magnetic field. Our work constitutes the first direct, ensemble-averaged study of microscopic magnetic return-point memory, and demonstrates the profound impact of interfacial roughness on this phenomenon. At low fields, the microscopic magnetic domains forget their past history with an exponential field dependence.

DOI: 10.1103/PhysRevLett.90.175502 PACS numbers: 61.10.–i, 07.85.Qe, 75.60.Ej, 78.70.Dm

The invention of the laser revolutionized visible optics. We are on the verge of a similar revolution in x-ray optics. Fully coherent, quasicontinuous beams of x rays are now available from the third-generation synchrotron sources, and extremely intense, fully coherent, pulsed beams from fourth-generation synchrotron sources are on the horizon. One of the most exciting applications is to use these coherent beams to do the x-ray analog of laser light scattering to study the spacetime correlations in materials at the nanoscopic and atomic length scales. Such coherent x-ray studies have achieved time resolutions from microseconds to nanoseconds at the few nanometer length scale [1]. Another promising application is to use the fourth-generation sources to do holographic or speckle x-ray imaging to determine the complete structure of the sample with atomic resolution using a single femtosecond duration beam pulse. Such ''lenseless speckle reconstruction'' has recently been demonstrated for x-ray charge scattering [2], and it is just beginning to be explored for x-ray magnetic scattering [3].

In this Letter, we describe a new form of reconstructionless x-ray speckle metrology using coherent, resonant, magnetic x-ray scattering. We show that the speckle patterns act as a fingerprint of the domain configurations and allow the ensemble of microscopic magnetic domains to be monitored versus the applied field history. By comparing speckle patterns, we obtain a quantitative measure of the domain evolution during the reversal process and directly probe the microscopic mechanisms of hysteresis. Magnetic hysteresis is fundamental to all magnetic storage technology, and this technology is one cornerstone of the present information age. Yet, despite decades of intense study [4] and significant recent advances [5], we still do not have a fully satisfactory microscopic understanding of magnetic hysteresis.

In his 1905 dissertation at Gottingen, Madelung defined macroscopic return-point memory (RPM) as follows: Suppose a magnetic system on the major hysteresis loop is subject to a change in the applied field that causes an excursion along a minor hysteresis loop inside the major loop; if the applied field is readjusted back to its original value and the sample returns to its initial magnetization, then macroscopic RPM is said to exist. Madelung's macroscopic characterization immediately raises the question of how the ferromagnetic domains behave on a microscopic level. Do the domains remember (i.e., return precisely to) their initial states, or does just the ensemble average remember? In agreement with previous qualitative studies [6], we find that our samples have perfect macroscopic RPM, but that they have imperfect microscopic RPM. In addition, we quantitatively measure the fraction of the domains that remember versus the applied field history and show that the roughness has a profound impact on the microscopic RPM.

In the past, microscopic RPM has primarily been studied using Barkhausen noise [7]. For some systems, there are extremely clear repetitions of the Barkhausen noise that indirectly indicate that there is microscopic RPM. However, other systems show only limited (or no) repetition. Barkhausen noise measurements indirectly probe the ensemble of the magnetic domains via the measured time structure of the spin-flip avalanches. In contrast, we use coherent x-ray magnetic scattering to directly probe the microscopic structure of the domains via the dynamic structure factor $S(\mathbf{Q}, \omega)$, which is the spacetime Fourier transform of the two-point correlation function of the magnetization density $\langle M(\mathbf{r}, t)M(\mathbf{0}, 0)\rangle$ inside the coherently illuminated region.

Our samples were grown on smooth, low-stress, 150-nm-thick SiN_x membranes by magnetron sputtering at different argon gas pressures. The multilayer structure of our two samples is identical

$$\text{Pt (20 nm) [Co (0.4 nm)/Pt (0.7 nm)]}_{50}\text{ Pt (1.5 nm)},$$

but their interfacial roughness increases with increased sputtering pressure. The sputtering pressure modifies the energies of the deposited atoms and alters the growth kinetics. In general, low-pressure sputtering results in smooth layers while high-pressure growth leads to cumulative roughness that evolves into domed columns with well defined grain boundaries [8]. Our goal is to study the microscopic RPM versus the roughness. The wo samples discussed here were grown at 3 and 12 mTorr with surface roughness, as determined by atomic force microscopy, of 0.45 and 0.90 nm rms, respectively. The major hysteresis loops measured with the applied field perpendicular to the film reflect the difference in the roughness and are shown in Fig. 1. The smooth, low-pressure sample (3 mT) exhibited reversal by nucleation and domain wall motion, and the shape of its major loop reflects the thin film geometry and the perpendicular anisotropy [9]. The rough, high-pressure sample (12 mT) exhibited much higher coercive fields as a direct consequence of the increased interfacial roughness. Kerr and SQUID measurements showed that both of our samples exhibited "perfect" macroscopic RPM.

Our experiments, performed at the Advanced Light Source at Lawrence Berkeley National Laboratory, use linearly polarized x rays from the third harmonic of the beam line 9 undulator [10]. The photon energy is set to the cobalt L_3 resonance at ~778 eV. To achieve transverse coherence, the raw undulator beam is passed through a 25-μm-diam pinhole before being scattered in transmission by the sample. The resonant magnetic scattering is collected by a soft x-ray charge-coupled device (CCD) camera. The magnetic domains are manipulated by an electromagnet, which applies fields perpendicular to the film. The intensity of the raw undulator beam is $\sim 2 \times 10^{14}$ photons/sec, that of the coherent beam is $\sim 2 \times 10^{12}$ photons/sec, and that of the scattered beam is $\sim 2 \times 10^{7}$ photons/sec. We collect data for 100 s at each magnetic field value, so our speckle patterns have a total of $\sim 2 \times 10^{9}$ photons in $\sim 10^{6}$ CCD pixels.

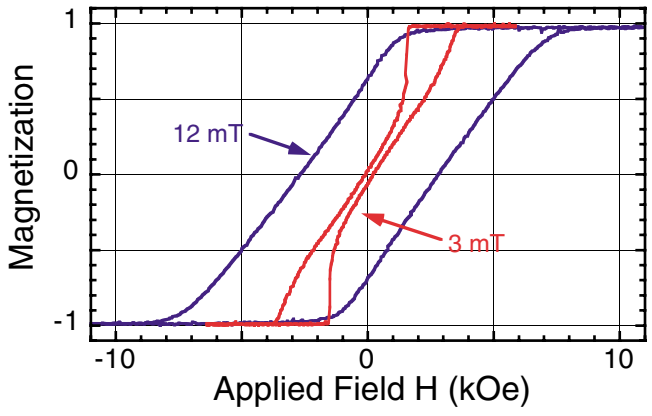

FIG. 1 (color online). Kerr measurements of the major loops for the samples grown at different argon sputtering pressures.

A typical magnetic speckle pattern for the 3 mT sample at zero applied field is shown in Fig. 2. The dominant structure is a ring of diffuse scattering reminiscent of the scattering from a classical $2d$ liquid exhibiting short-range positional correlations. Note that this diffuse scattering is strongly speckled due to our use of transversely coherent x rays. Since changes in the domain structure will produce changes in the speckle pattern, the degree of

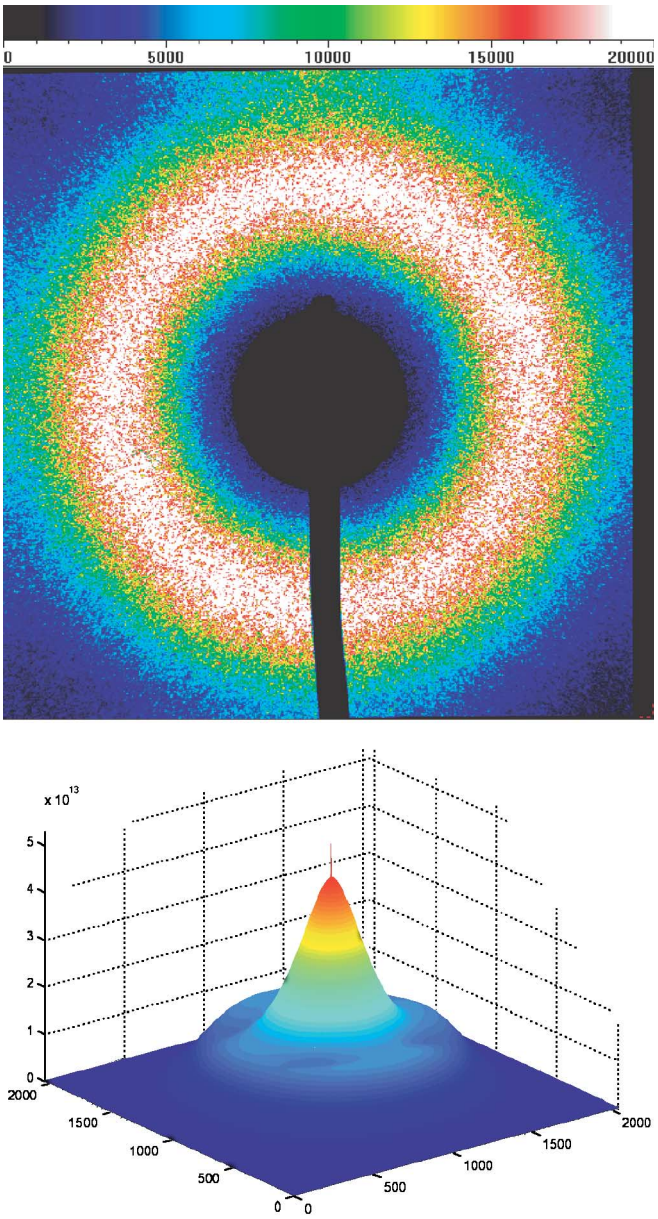

FIG. 2 (color online). X-ray metrology for the 3 mT sample. Top: the measured speckle pattern at zero field. Bottom: the calculated autocorrelation function. Our CCD has 1024 by 1024 pixels; the autocorrelation function is plotted in terms of 2047 by 2047 pixels. The very sharp spike in the center is a few pixels wide and is due to the speckles produced by the coherent scattering; the broad mountain under the coherent spike is hundreds of pixels wide and is due to the smooth average (incoherent) scattering.

microscopic RPM can be precisely measured by cross correlating different speckle patterns. By converting the auto- and cross-correlation functions into a normalized correlation coefficient, we can obtain a precise measure of the degree of cross correlation between the domains without performing an explicit "speckle reconstruction." Note that even if we did perform a speckle reconstruction, or directly measured the magnetic domains using an imaging technique, we would still need to reduce the total amount of information down to a reasonable size to produce a compact, convenient, ensemble-averaged measure of the microscopic RPM. To do so, we have chosen the simplest scalar measure of the changes in the speckle pattern, which is given by a correlation coefficient. As usual, x-ray diffraction and high-resolution imaging are complementary probes; diffraction offers a very convenient way to obtain an ensemble average; imaging provides the best information about individual domains and defects.

To quantify the correlation between two speckle patterns, we generalized the standard correlation coefficient for two random variables a and b, which is given by

$$\rho(a, b) = \mathrm{Cov}(a, b) \times \{\mathrm{Var}(a)\mathrm{Var}(b)\}^{-1/2},$$

to the analogous expression in terms of the cross-correlation function (CCF) and the autocorrelation functions (ACF) of the speckle pattern intensities $A(q_x, q_y)$ and $B(q_x, q_y)$

$$\rho(A, B) = \sum[\mathrm{CCF}(A, B) - D] \times \left\{\sum[\mathrm{ACF}(A) - E]\sum[\mathrm{ACF}(B) - F]\right\}^{-1/2}.$$

In order to collect all of the speckle information, which is spread over several pixels because our speckles are 2–3 pixels wide, we first sum over the pixels near the center of the auto- or cross-correlation function which contain the speckle information, and we then subtract the incoherent background levels [i.e., $D(q_x, q_y)$, $E(q_x, q_y)$, and $F(q_x, q_y)$] from each one. Our generalized correlation coefficient ρ is unity for identical speckle patterns, and is zero when the patterns are completely uncorrelated. In general, the value of ρ specifies the degree of correlation between the two speckle patterns which in turn are proportional to the Fourier coefficients of the magnetization density for the two magnetic domain configurations. A typical example of one of our experimental autocorrelation functions is shown in Fig. 2.

The first question that we addressed was whether our samples exhibited microscopic RPM through magnetic saturation. To do so, we compared two speckle patterns collected at the same point on the major loop, but separated either by a minor loop that returned to saturation or by one or more full excursions around the major loop. For our smooth 3 mT sample, we found no correlation ($\rho = 0$) for speckle patterns separated by a return to saturation. For our rough 12 mT sample, we found that there was a repeatable correlation with $\rho \sim 0.2$–0.6 between the speckle patterns at a given magnetic field separated by one or even by many complete major loops.

Since our smooth 3 mT sample did not have microscopic RPM through saturation, we measured the decay of its microscopic RPM as it approached magnetic saturation to determine how it forgets. Our results are shown in Fig. 3. For each field H, we measured five speckle patterns which were prepared using the following magnetic field history protocol: (0) -10 kOe (negative saturation), (1) H, (2) H, (3) 0 kOe, and (4) H. The negative saturation speckle pattern was used to determine the background scattering; $\rho(1, 2)$ was used to test for any slow time dependence of the speckle patterns at that field value; $\rho(2, 3)$ was used to determine the irreversible component of the domain magnetization—this is analogous to the standard macroscopic measurement of the remanence magnetization to separate the reversible and irreversible components of the macroscopic magnetization; $\rho(2, 4)$ was used to determine the total (reversible plus irreversible) component of the domain magnetization. We calculated the normalized reversible and irreversible fractional changes via $F(\mathrm{rev}) = [\rho(2, 4) - \rho(2, 3)]/\rho(1, 2)$ and $F(\mathrm{irrev}) = [\rho(1, 2) - \rho(2, 3)]/\rho(1, 2)$.

Figure 3 shows two different kinds of relaxation of the magnetic domains (1) a field-dependent, quasistatic relaxation at low fields, and (2) a time-dependent, field-dependent relaxation at high fields. Below 2 kOe, $\rho(1, 2)$ remains near unity and both $\rho(2, 3)$ and $\rho(2, 4)$ show a field-dependent, quasistatic, exponential deviation from unity. This confirms the absence of instrumental drift in our measurements and shows that the magnetic domain structure is static during the several minutes required to collect the data. Above 2 kOe, the monotonic decrease in $\rho(1, 2)$ reveals a time-dependent, field-dependent relaxation of the magnetic domains. Note that the reversible

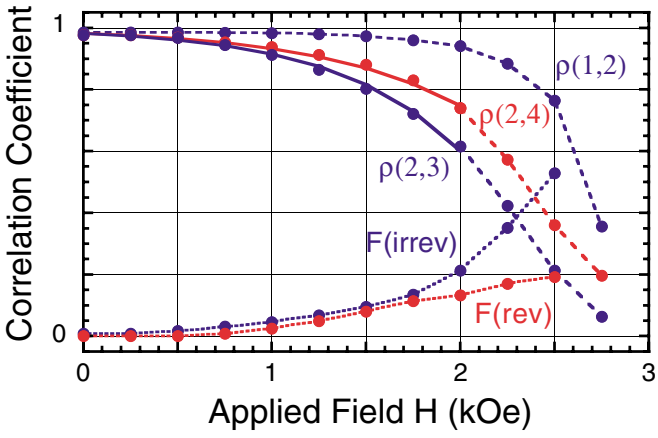

FIG. 3 (color online). The measured minor loop microscopic correlation coefficients for the 3 mT sample. The solid lines represent fits to exponential deviations from unity. The dashed lines are guides to the eye.

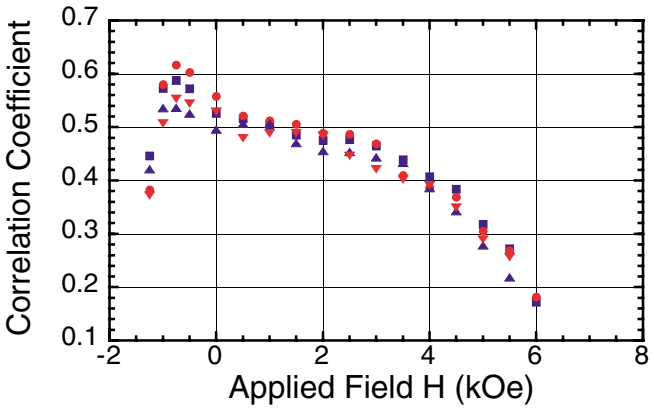

FIG. 4 (color online). The measured major loop microscopic correlation coefficients for the 12 mT sample. The circles and squares (the triangles) represent the correlations between the first and the second (eleventh) loop.

and irreversible fractional changes are essentially zero near zero field, and that both increase for higher field values.

For our rough 12 mT sample, we measured the correlation coefficient for pairs of points at the same applied field value on the major loop which were separated by either one complete major loop or by 11 complete major loops. As shown in Fig. 4, this sample exhibits repeatable major loop microscopic RPM with $\rho \sim 0.2$–0.6 depending on the applied field value. This demonstrates that sufficient interfacial roughness produces partial major loop microscopic RPM. We find the highest ρ values near the nucleation point for reversal and a systematic decrease in ρ toward saturation. This suggests that the same nucleation points initiate the reversal, but that the domain structure becomes increasingly uncorrelated as the reversal progresses because different reversal pathways are sampled by the system.

Our results are the first detailed, ensemble-averaged measurements of the decay of the microscopic RPM in magnetic materials. For our smooth sample, saturation completely destroyed the microscopic RPM. For our rough sample, saturation only partially destroyed the microscopic RPM. The theoretical studies of microscopic RPM have focused on the behavior of zero-temperature random field Ising models (RFIM) which have perfect major and minor loop microscopic RPM [5]. It will be very interesting to see if the exponential decays of the microscopic RPM that we find in our experiments emerge in a natural way from either the finite-temperature RFIMs [5] or the theories for perpendicular magnetic systems [9].

In addition to ferromagnets, there is a wide variety of materials that exhibit hysteresis and memory effects for which we do not yet have a satisfactory microscopic understanding, for example, ferroelectrics [11], spin glasses [12], and shape memory materials [13]. The coherent x-ray scattering cross-correlation method that we have developed can also be used to study the microscopic memory in these systems. In addition to the quasistatic behavior that we have addressed here, coherent x-ray magnetic scattering can also be used to study the incoherent, thermally driven dynamics of the microscopic domains [1].

We gratefully acknowledge the support of our work by the U.S. DOE via DE-FG06-86ER45275, DE-AC03-76SF00098, and DE-FG03-99ER45776. O. H. was partially supported by the Deutsche Forschungsgemeinschaft via HE 3286/1-1.

[1] A. C. Price *et al.*, Phys. Rev. Lett. **82**, 755 (1999); I. Sikharulidze *et al.*, Phys. Rev. Lett. **88**, 115503 (2002).
[2] See, for example, J. Miao and D. Sayre, Acta Crystallogr. Sect. A **56**, 596 (2000); I. A. Vartanyants and I. K. Robinson, J. Phys. Condens. Matter **13**, 10 593 (2001); U. Weierstall *et al.*, Ultramicroscopy **90**, 171 (2002), and references therein.
[3] T. O. Mentes, C. Sanchez-Hanke, and C. C. Kao, J. Synchrotron Radiat. **9**, 90 (2002); F. Yakhou *et al.*, J. Magn. Magn. Mater. **233**, 119 (2001); A. Rahmim, M.S. thesis, University of British Columbia, 2001.
[4] See, for example, G. Bertotti, *Hysteresis in Magnetism* (Academic, San Diego, 1998); M. Brokate and J. Sprekels, *Hysteresis and Phase Transitions* (Springer, New York, 1996); E. Della Torre, *Magnetic Hysteresis* (IEEE Press, New York, 1999).
[5] See, for example, J. P. Sethna, K. A. Dahmen, and C. R. Myers, Nature (London) **410**, 242 (2001); J. H. Carpenter *et al.*, J. Appl. Phys. **89**, 6799 (2001); K. A. Dahmen *et al.*, J. Magn. Magn. Mater. **226–230**, 1287 (2001); K. A. Dahmen, J. P. Sethna, and O. Perkovic, IEEE Trans. Magn. **36**, 3150 (2000), and references therein.
[6] See, for example, H. S. Cho *et al.*, IEEE Trans. Magn. **34**, 1150 (1998); A. Hulbert and R. Schaefer, in *Magnetic Domains* (Springer, Berlin, 1998), Sec. 5.6.1.P. Fischer *et al.*, J. Phys. D **31**, 649 (1998).
[7] S. Zapperi and G. Durin, Comput. Mater. Sci. **20**, 436 (2001); J. R. Petta, M. B. Weissman, and G. Durin, Phys. Rev. E **56**, 2776 (1997); D. Spasojevic *et al.*, Phys. Rev. E **54**, 2531 (1996).
[8] E. E. Fullerton *et al.*, Phys. Rev. B **48**, 17 432 (1993).
[9] C. Kooy and C. Enz, Philips Res. Rep. **15**, 7 (1960); Y. Yafet and E. M. Gyorgi, Phys. Rev. B **38**, 9145 (1988); B. Kaplan and G. A. Gehring, J. Magn. Magn. Mater. **128**, 111 (1993); A. Kashuba and V. L. Pokrovsky, Phys. Rev. Lett. **70**, 3155 (1993); Phys. Rev. B **48**, 10 335 (1993).
[10] J. B. Kortright *et al.*, Phys. Rev. B **64**, 092401 (2001); B. Hu *et al.*, Synchrotron Radiation News **14**, 11 (2001).
[11] E. V. Colla, L. K. Chao, and M. B. Weissman, Phys. Rev. Lett. **88**, 017601 (2002); Phys. Rev. B **63**, 134107 (2001).
[12] M. B. Weissman, Physica (Amsterdam) **107D**, 421 (1997); Rev. Mod. Phys. **65**, 829 (1993).
[13] L. Carrillo and J. Ortin, Phys. Rev. B **56**, 11 508 (1997).